further contribute to an understanding of the biology of AN.

REFERENCES

Aberle J, Fedderwitz I, Klages N, George E, Beil FU. 2007. Genetic variation in two proteins of the endocannabinoid system and their influence on body mass index and metabolism under low fat diet. Horm Metab Res 39:395–397.

Aberle J, Flitsch J, Beck NA, Mann O, Busch P, Peitsmeier P, Beil FU. 2008. Genetic variation may influence obesity only under conditions of diet: Analysis of three candidate genes. Mol Genet Metab 95:188–191.

Baker D, Pryce G, Davies WL, Hiley CR. 2006. In silico patent searching reveals a new cannabinoid receptor. Trends Pharmacol Sci 27:1–4.

Berkman ND, Lohr KN, Bulik CM. 2007. Outcomes of eating disorders: A systematic review of the literature. Int J Eat Disord 40:293–309.

Bulik CM, Sullivan PF, Tozzi F, Furberg H, Lichtenstein P, Pedersen NL. 2006. Prevalence, heritability, and prospective risk factors for anorexia nervosa. Arch Gen Psychiatry 63:305–312.

Capasso R, Izzo AA. 2008. Gastrointestinal regulation of food intake: General aspects and focus on anandamide and oleoylethanolamide. J Neuroendocrinol 20 (Suppl 1):39–46.

Cooper SJ. 2004. Endocannabinoids and food consumption: Comparisons with benzodiazepine and opioid palatability-dependent appetite. Eur J Pharmacol 500:37–49.

Dixon AL, Liang L, Moffatt MF, Chen W, Heath S, Wong KC, Taylor J, Burnett E, Gut I, Farrall M, Lathrop GM, Abecasis GR, Cookson WO. 2007. A genome-wide association study of global gene expression. Nat Genet 39:1202–1207.

Fride E, Ginzburg Y, Breuer A, Bisogno T, Di Marzo V, Mechoulam R. 2001. Critical role of the endogenous cannabinoid system in mouse pup suckling and growth. Eur J Pharmacol 419:207–214.

Fride E, Foox A, Rosenberg E, Faigenboim M, Cohen V, Barda L, Blau H, Mechoulam R. 2003. Milk intake and survival in newborn cannabinoid CB1 receptor knockout mice: Evidence for a "CB3" receptor. Eur J Pharmacol 461:27–34.

Frieling H, Albrecht H, Jedtberg S, Gozner A, Lenz B, Wilhelm J, Hillemacher T, de Zwaan M, Kornhuber J, Bleich S. 2009. Elevated cannabinoid 1 receptor mRNA is linked to eating disorder related behavior and attitudes in females with eating disorders. Psychoneuroendocrinology 34:620–624.

Gaetani S, Kaye WH, Cuomo V, Piomelli D. 2008. Role of endocannabinoids and their analogues in obesity and eating disorders. Eat Weight Disord 13:e42–e48.

Grigoroiu-Serbanescu M, Magureanu S, Milea S, Dobrescu I, Marinescu E. 2003. Modest familial aggregation of eating disorders in restrictive anorexia nervosa with adolescent onset in a Romanian sample. Eur Child Adolesc Psychiatry 12 (Suppl 1):I47–I53.

Hao S, Avraham Y, Mechoulam R, Berry EM. 2000. Low dose anandamide affects food intake, cognitive function, neurotransmitter and corticosterone levels in diet-restricted mice. Eur J Pharmacol 392:147–156.

Harrold JA, Williams G. 2003. The cannabinoid system: A role in both the homeostatic and hedonic control of eating? Br J Nutr 90:729–734.

Henstridge CM, Balenga NA, Ford LA, Ross RA, Waldhoer M, Irving AJ. 2009. The GPR55 ligand L-{alpha}-lysophosphatidylinositol promotes RhoA-dependent Ca2+ signaling and NFAT activation. FASEB J 23:183–193.

Herzog DB, Franko DL, Dorer DJ, Keel PK, Jackson S, Manzo MP. 2006. Drug abuse in women with eating disorders. Int J Eat Disord 39:364–368.

Iacovino JR. 2004. Anorexia nervosa: A 63-year population-based survival study. J Insur Med 36:107–110.

Karwautz A, Troop NA, Rabe-Hesketh S, Collier DA, Treasure JL. 2003. Personality disorders and personality dimensions in anorexia nervosa. J Personal Disord 17:73–85.

Kirkham TC. 2005. Endocannabinoids in the regulation of appetite and body weight. Behav Pharmacol 16:297–313.

Klump KL, Gobrogge KL. 2005. A review and primer of molecular genetic studies of anorexia nervosa. Int J Eat Disord 37 (Suppl): S43–S48; discussion S87–S49.

Klump KL, Bulik CM, Pollice C, Halmi KA, Fichter MM, Berrettini WH, Devlin B, Strober M, Kaplan A, Woodside DB, Treasure J, Shabbout M, Lilenfeld LR, Plotnicov KH, Kaye WH. 2000. Temperament and character in women with anorexia nervosa. J Nerv Ment Dis 188:559–567.

Klump KL, Strober M, Bulik CM, Thornton L, Johnson C, Devlin B, Fichter MM, Halmi KA, Kaplan AS, Woodside DB, Crow S, Mitchell J, Rotondo A, Keel PK, Berrettini WH, Plotnicov K, Pollice C, Lilenfeld LR, Kaye WH. 2004. Personality characteristics of women before and after recovery from an eating disorder. Psychol Med 34:1407–1418.

Lauckner JE, Jensen JB, Chen HY, Lu HC, Hille B, Mackie K. 2008. GPR55 is a cannabinoid receptor that increases intracellular calcium and inhibits M current. Proc Natl Acad Sci USA 105:2699–2704.

Logue CM, Crowe RR, Bean JA. 1989. A family study of anorexia nervosa and bulimia. Compr Psychiatry 30:179–188.

Mazzeo SE, Mitchell KS, Bulik CM, Reichborn-Kjennerud T, Kendler KS, Neale MC. 2009. Assessing the heritability of anorexia nervosa symptoms using a marginal maximal likelihood approach. Psychol Med 39:463–473.

Molgaard CA, Chambers CM, Golbeck AL, Elder JP, Ferguson J. 1989. Maternal alcoholism and anorexia nervosa: a possible association? Int J Addict 24:167–173.

Monteleone P, Matias I, Martiadis V, De Petrocellis L, Maj M, Di Marzo V. 2005. Blood levels of the endocannabinoid anandamide are increased in anorexia nervosa and in binge-eating disorder, but not in bulimia nervosa. Neuropsychopharmacology 30:1216–1221.

Monteleone P, Bifulco M, Di Filippo C, Gazzerro P, Canestrelli B, Monteleone F, Proto MC, Di Genio M, Grimaldi C, Maj M. 2009. Association of CNR1 and FAAH endocannabinoid gene polymorphisms with anorexia nervosa and bulimia nervosa: evidence for synergistic effects. Genes Brain Behav 8:728–732.

Muller TD, Reichwald K, Bronner G, Kirschner J, Nguyen TT, Scherag A, Herzog W, Herpertz-Dahlmann B, Lichtner P, Meitinger T, Platzer M, Schafer H, Hebebrand J, Hinney A. 2008. Lack of association of genetic variants in genes of the endocannabinoid system with anorexia nervosa. Child Adolesc Psychiatry Ment Health 2:33.

Oka S, Nakajima K, Yamashita A, Kishimoto S, Sugiura T. 2007. Identification of GPR55 as a lysophosphatidylinositol receptor. Biochem Biophys Res Commun 362:928–934.

Redgrave GW, Coughlin JW, Heinberg LJ, Guarda AS. 2007. First-degree relative history of alcoholism in eating disorder inpatients: Relationship to eating and substance use psychopathology. Eat Behav 8:15–22.

Rodondi N, Pletcher MJ, Liu K, Hulley SB, Sidney S. 2006. Marijuana use, diet, body mass index, and cardiovascular risk factors (from the CARDIA study). Am J Cardiol 98:478–484.

Ryberg E, Larsson N, Sjogren S, Hjorth S, Hermansson NO, Leonova J, Elebring T, Nilsson K, Drmota T, Greasley PJ. 2007. The orphan receptor GPR55 is a novel cannabinoid receptor. Br J Pharmacol 152:1092–1101.

Siegfried Z, Kanyas K, Latzer Y, Karni O, Bloch M, Lerer B, Berry EM. 2004. Association study of cannabinoid receptor gene (CNR1) alleles and anorexia nervosa: Differences between restricting and binging/purging subtypes. Am J Med Genet B Neuropsychiatr Genet 125B:126–130.

Slof-Op 't Landt MC, van Furth EF, Meulenbelt I, Slagboom PE, Bartels M, Boomsma DI, Bulik CM. 2005. Eating disorders: From twin studies to candidate genes and beyond. Twin Res Hum Genet 8:467–482.

Strober M, Freeman R, Lampert C, Diamond J, Kaye W. 2000. Controlled family study of anorexia nervosa and bulimia nervosa: Evidence of shared liability and transmission of partial syndromes. Am J Psychiatry 157:393–401.

Toth A, Blumberg PM, Boczan J. 2009. Anandamide and the vanilloid receptor (TRPV1). Vitam Horm 81:389–419.

Wade TD, Bulik CM, Neale M, Kendler KS. 2000. Anorexia nervosa and major depression: Shared genetic and environmental risk factors. Am J Psychiatry 157:469–471.

Wierzbicki AS. 2006. Rimonabant: Endocannabinoid inhibition for the metabolic syndrome. Int J Clin Pract 60:1697–1706.

Williams CM, Rogers PJ, Kirkham TC. 1998. Hyperphagia in pre-fed rats following oral delta9-THC. Physiol Behav 65:343–346.

PEDIATRICS INTERNATIONAL Official Journal of the Japan Pediatric Society

Pediatrics International (2010) **52**, e150–e153 doi: 10.1111/j.1442-200X.2010.03073.x

Patient Report

Case of glycogen storage disease type VI (phosphorylase deficiency) complicated by focal nodular hyperplasia

Atsushi Ogawa,[1] Emi Ogawa,[1] Shigenori Yamamoto,[1] Tokiko Fukuda,[2] Hideo Sugie[2] and Yoichi Kohno[1]

[1]*Department of Pediatrics, Chiba University Graduate School of Medicine, Chiba-shi, Chiba and* [2]*Department of Pediatrics, Jichi Children's Medical Center Tochigi, Shimotsuke-shi, Tochigi, Japan*

Key words focal nodular hyperplasia, glycogen phosphorylase, glycogen storage disease.

Although it is well known that hepatic tumors often develop in patients with glycogen storage disease (GSD) types Ia and III, the formation of these tumors has not been reported in other forms of hepatic GSD. In this report, a patient with GSD type VI (phosphorylase deficiency; OMIM 232700) complicated with a hepatic benign tumor, focal nodular hyperplasia (FNH), is presented. This case indicates that regular check-ups for hepatic tumors are necessary, not only in patients with GSD types Ia or III, but also in patients with other forms of hepatic GSD.

Case Report

A female patient was referred to our hospital when she was 5 years of age for further investigation of hepatomegaly, which had been detected when she had visited a clinic when she was 5 years old. She was born to healthy non-consanguineous parents and had no history of hypoglycemia or nasal bleeding. On physical examination, her height was 101 cm (−1.5 SD) and her bodyweight was 16 kg (−1.0 SD). The liver was firm and palpable 7 cm below the right costal margin, whereas the spleen was not palpable. The results of a fasting blood test collected at that time were as follows: aspartate aminotransferase 37U/L, alanine aminotransferase 24U/L, blood glucose 85 mg/dL, lactate 6.2 mg/dL, uric acid 5.9 mg/dL, total cholesterol 229 mg/dL and triglyceride 88 mg/dL. A plain abdominal computed tomography (CT) scan showed an enlarged liver with a density considerably higher than that of the spleen (CT values: liver, 80; spleen, 42) (Fig. 1). Glucose and galactose loading tests were performed. The serum lactate level was not elevated when glucose was loaded, although it increased to a maximum of 56 mg/dL one hour after loading (normal <35 mg/dL). A glucagon loading test was performed after a 15-h fast, with the serum glucose level increasing from 71 to 128 mg/dL one hour after loading. On the basis of these data, GSD was suspected and accordingly the enzyme activities of hepatic GSD, that is, debranching enzyme, phosphorylase and phosphorylase b kinase, were measured in peripheral blood. The results of all these tests were normal (Table 1). Informed consent for a liver needle biopsy for measurement of enzyme activity was not obtained. Although the enzyme activity of phosphorylase b kinase measured in peripheral blood was normal, a tentative diagnosis of GSD type IX (phosphorylase b kinase deficiency) was made based on the physical, laboratory and radiological findings and the results of the loading tests. Regular check-ups including abdominal CT scans for potential formation of hepatic tumor were performed every year. The patient's growth curve showed that she attained mean values around the time of puberty. The results of blood tests obtained between 5 and 14 years of age were as follows (mean ± SD): uric acid 5.9 ± 0.6 mg/dL, total cholesterol 208 ± 21.0 mg/dL and triglyceride 198 ± 111 mg/dL.

When the patient was 15 years of age, the early phase of a contrast-enhanced abdominal CT scan revealed an enhanced lesion in the liver (Fig. 1). After obtaining informed consent, specimens were obtained by needle biopsy from the tumor and non-tumor part of the liver. Histological findings of the non-tumor specimen showed strong periodic acid-Schiff (PAS) staining in hepatocytes that disappeared following diastase treatment, findings compatible with GSD. Histology of the tumor specimen demonstrated pericellular fibrosis, compatible with the diagnosis of FNH (Fig. 2). Fibrous bands containing bile ductules were not observed in the specimens. Enzyme activities of hepatic GSD were measured using liver tissue from the non-tumor section, which revealed that phosphorylase enzyme activity was 2.3 nmol/min/mg protein, a value corresponding to 24% of normal. The enzyme activity of both debranching enzyme and phosphorylase b kinase was normal (Table 1). Informed consent for gene analysis of phosphorylase (*PGYL*) could not be obtained. We concluded that the patient's diagnosis was GSD VI (phosphorylase deficiency) complicated by FNH. We elected to forego surgical treatment in favor of long-term observation. The size of the tumor has been monitored regularly with ultrasonography. As of now, the tumor does not appear to be enlarging.

Discussion

In this report we present a patient with GSD type VI complicated by FNH. This is the first report of a hepatic tumor complication

Correspondence: Atsushi Ogawa, MD PhD, Department of Pediatrics, Chiba University Graduate School of Medicine, 1-8-1 Inohana, Chuo-ku, Chiba 260-8670, Japan. Email: aogawa@faculty.chiba-u.jp

Received 28 February 2009; revised 7 June 2009; accepted 9 July 2009.

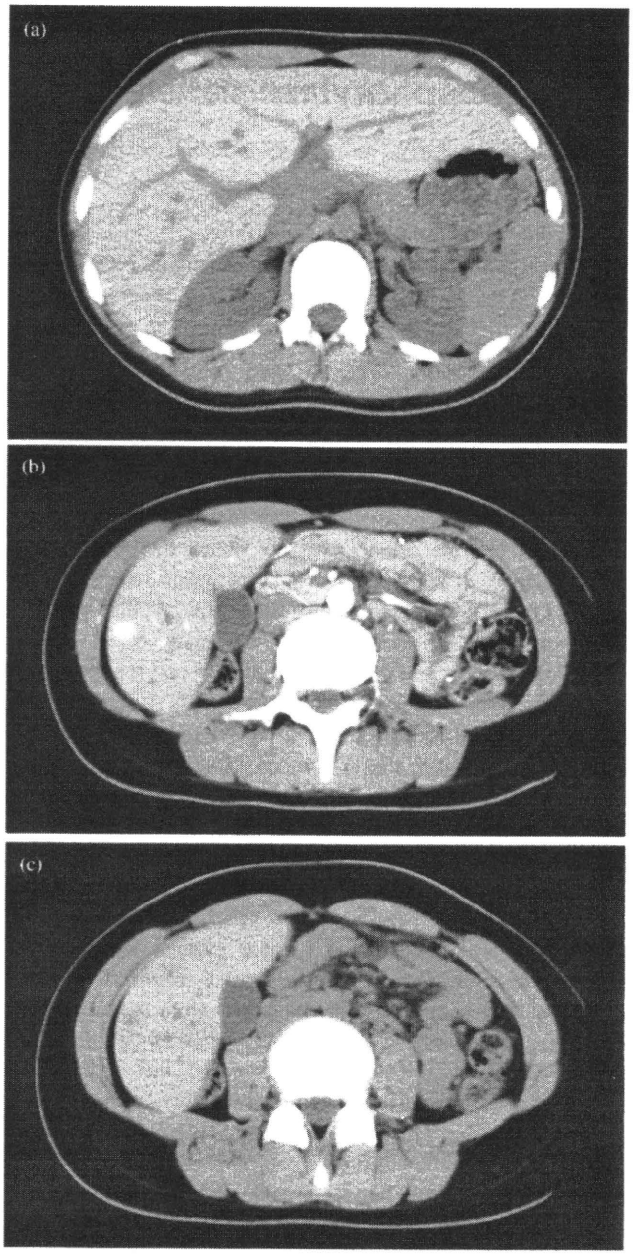

Fig. 1 (a) The findings of a plain abdominal computed tomography (CT) scan at 5 years of age. The CT value of the liver was markedly elevated compared with that of the spleen and kidneys. (b) The findings of the early phase of a contrast-enhanced abdominal CT scan at 15 years of age showing an enhanced lesion. (c) The findings of the same section as (b), without contrast enhancement.

in a patient with GSD type VI, a different hepatic form of GSD than types Ia or III. As hepatic tumors are often found in patients with GSD types Ia and III, regular check-ups for these tumors are performed routinely in these patients. However, this report indicates that regular check-ups for hepatic tumor are also necessary in patients with hepatic forms of GSD other than types Ia or III.

In patients with GSD type Ia, hepatic adenoma is the most common tumor described; however other tumors, including hepatocellular carcinoma (HCC),[1] described in patients with GSD III,[2] hepatoblastomas,[3] and FNH[4] have also been reported.

Hepatic adenomas are a benign tumor, consisting of a nodular proliferation of hepatocytes arranged in cords having no relationship to portal tracts. They often have a pushing border abutting against the surrounding liver. The hepatic adenoma has, on rare occasions, been known to progress to HCC,[1] and this is one of the most important reasons why regular check-ups and follow up after the discovery of an adenoma are necessary in a patient with GSD Ia. FNH is typically a single mass in an otherwise healthy liver characterized by central scarring that radiates between multiple nodules of regenerating parenchyma. Like the hepatic adenoma, it is also a benign tumor parenchyma but the potential for malignant transformation of FNH into HCC has not been demonstrated. However, a case of HCC arising within FNH has been reported recently[5] and this report emphasizes the importance of detecting FNH, even though the FNH itself is benign.

The mechanism of tumor formation in GSD type Ia is considered to occur by the following sequence.[6] Increased amounts of free fatty acids are released from adipose tissue, taken up by the liver and channeled into triglyceride formation. Malonyl-CoA is a key lipogenic intermediate in this process, which, in turn, causes inhibition of carnitine palmitoyltransferase I and limitation of mitochondrial beta-oxidation. This results in fatty acids being more likely to be channeled into extramitochondrial pathways, such as within peroxisomes, leading to an increase in hydrogen peroxide generation. This results in increased generation of free radicals that are capable of inflicting direct DNA damage, which may initiate the development of hepatic tumors. Although the patient reported here was diagnosed with GSD type VI, hypertriglyceridemia was almost always observed during the clinical course of the disease, similar to that seen in cases with type I GSD. We anticipate this would have resulted in increased generation of free radicals by the mechanism described above and could possibly have caused the formation of FNH we observed in the patient.

In our patient we observed a difference in phosphorylase activity between peripheral blood and liver tissue. Three isoforms of phosphorylase exist, that is, liver, brain and muscle. As the liver isoform is expressed in peripheral blood,[7,8] phosphorylase activity in peripheral blood and the liver should be the same. The reason why phosphorylase activity in peripheral blood and liver was different in our patient is not clear, although similar findings have been reported elsewhere.[9] Mutation analysis of the liver glycogen phosphorylase gene (*PYGL*) is necessary for further confirmation of this diagnosis.

In summary, we report a patient with GSD VI complicated with FNH. This case indicates that regular check-ups for hepatic tumors are necessary, not only in patients with GSD types Ia or III, but also in patients with other forms of hepatic GSD.

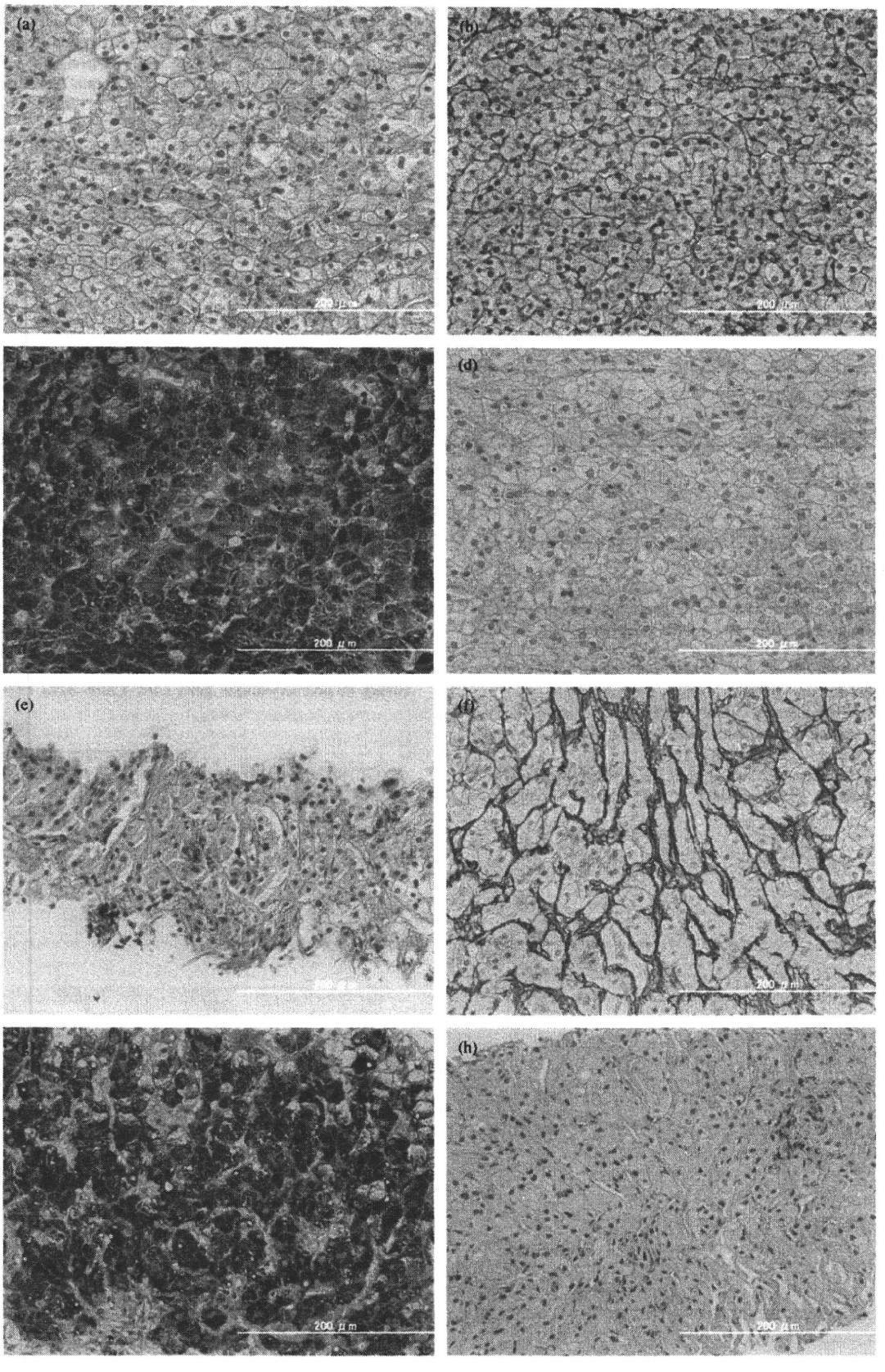

Fig. 2 Histological findings of the liver from (a–d) non-tumor and (e–h) tumor specimens. (a and e) Hematoxylin–eosin (HE) stain, (b and f) silver staining, (c and g) periodic acid-Schiff (PAS) staining and (d and h) PAS staining after diastase treatment. In the non-tumor specimen, the hepatocytes had (a) clear cytoplasm with (b) no fibrosis observed. (c and d) All the hepatocytes were stained strongly by PAS, which disappeared following diastase treatment. (e and f) In tumor specimens, pericellular fibrosis was observed, whereas fibrous bands in which bile ductules were proliferating were not. On the basis of the finding of pericellular fibrosis, a diagnosis of focal nodular hyperplasia was made. The original magnification was ×20.

Table 1 Results of enzyme activity measurements in the patient and controls

Peripheral blood	Patient	Control 1	Control 2	
Debranching enzyme	14.8	24.9	19.1	Nmole glucose/hour/mg
Phosphorylase	6.3	6.1	7.2	Nmole/min/mg
Phosphorylase b kinase	45.8	44.5	42.0	Nmole/min/g Hb
Liver	**Patient**	**Controls**		
Debranching enzyme	243.4	197.4 ± 32.8 (n = 10)		Nmole glucose/hour/mg
Phosphorylase	2.3	9.6 ± 1.7 (n = 10)		Nmole/min/mg
Phosphorylase b kinase	49.6	62.7 ± 11.8 (n = 9)		Nmole/min/mg

References

1 Franco LM, Krishnamurthy V, Bali D *et al.* Hepatocellular carcinoma in glycogen storage disease type Ia: A case series. *J. Inherit. Metab. Dis.* 2005; **28**: 153–62.

2 Demo E, Frush D, Gottfried M *et al.* Glycogen storage disease type III-hepatocellular carcinoma a long-term complication? *J. Hepatol.* 2007; **46**: 492–8.

3 Ito E, Sato Y, Kawauchi K *et al.* Type Ia glycogen storage disease with hepatoblastoma in siblings. *Cancer* 1987; **59**: 1776–80.

4 Takamura M, Mugishima H, Oowada M, Harada K, Uchida T. Type La glycogen storage disease with focal nodular hyperplasia in siblings. *Acta Paediatr. Jpn.* 1995; **37**: 510–3.

5 Petsas T, Tsamandas A, Tsota I *et al.* A case of hepatocellular carcinoma arising within large focal nodular hyperplasia with review of the literature. *World J. Gastroenterol.* 2006; **12**: 6567–71.

6 Lee PJ. Glycogen storage disease type I: Pathophysiology of liver adenomas. *Eur. J. Pediatr.* 2002; **161**(Suppl 1): S46–9.

7 Proux D, Dreyfus JC. Phosphorylase isoenzymes in tissues: Prevalence of the liver type in man. *Clin. Chim. Acta* 1973; **48**: 167–72.

8 Proux D, Vibert M, Meienhofer MC, Dreyfus JC. The isozymes of glycogen phosphorylase in human and rabbit tissues. II. Electrofocusing in polyacrylamide gels. *Clin. Chim. Acta* 1974; **57**: 211–6.

9 Burwinkel B, Bakker HD, Herschkovitz E, Moses SW, Shin YS, Kilimann MW. Mutations in the liver glycogen phosphorylase gene (PYGL) underlying glycogenosis type VI. *Am. J. Hum. Genet.* 1998; **62**: 785–91.

ELSEVIER

Brain & Development 32 (2010) 356–361

BRAIN & DEVELOPMENT
Official Journal of the Japanese Society of Child Neurology

www.elsevier.com/locate/braindev

Original article

Study of *HOXD* genes in autism particularly regarding the ratio of second to fourth digit length

Yoko Sugie [a,*], Hideo Sugie [b], Tokiko Fukuda [b], Junko Osawa [a]

[a] *Department of Pediatrics, Hamamatsu University School of Medicine, Hamamatsu, Shizuoka, Japan*
[b] *Department of Pediatrics, Jichi Medical University and Jichi Children's Medical Center, Tochigi, Japan*

Received 30 December 2008; received in revised form 14 May 2009; accepted 16 May 2009

Abstract

Multiple genes are involved in the pathogenesis of autism. To study the causative gene, the relationship between autism endophenotypes and their closely related genes has been analyzed. There is a subgroup of autism spectrum disorder (ASD) in which the ratio of second digit length to fourth digit length (2D/4D) is low (short digit group, SDG). We studied the relationship between ASD and *HOXD* genes, which are located in the candidate locus for ASD and are associated with digit morphogenesis, with a particular focus on SDG. We analyzed 25 SNPs of *HOXD11*, *HOXD12*, and *HOXD13* in the subject of 98 ASD, 89 healthy controls, and 16 non-autistic patients (non-ASD). There was no significant difference in the genotype frequencies between the ASD and the healthy controls. However, the G-112T heterozygote in the promoter region of *HOXD11* was observed in only four patients with ASD and in none of the healthy controls or non-ASD subjects. Moreover, this *HOXD11* G-112T was observed in three of 11 SDG with ASD but in none of the 15 non-SDG patients with ASD. There were eight SDG patients among the non-ASD ones, but this polymorphism was observed in none of them. Considering the above results, it is expected that candidate genes will be further identified, using *HOXD11* G-112T polymorphism as a marker, by analyzing genes located near 2q in a larger number of ASD subjects with clinical signs of SDG.

Keywords: Autism; *HOXD*; 2D/4D; Endophenotype; Genetic polymorphism

This research was partly supported by a Grant-in-Aid for the Mentally and Physically Handicapped from the Ministry of Health, Labor and Welfare and the research Grant (14B-4-17) for Nervous and Mental Disorders from the Ministry of Health, Labor and Welfare, Japan. The authors declare that they have no competing interests.

* Corresponding author. Address: Department of Pediatrics, Hamamatsu University School of Medicine, 1-20-1, Handayama, Higashi-ku, Hamamatsu 431-3192, Japan. Tel.: +81 53 435 2312; fax: +81 53 435 4311.

E-mail addresses: y-sugie@umin.ac.jp (Y. Sugie), sugie@jichi.ac.jp (H. Sugie), toki-fukuda@jichi.ac.jp (T. Fukuda), yusosawa@nifty.com (J. Osawa).

0387-7604/$ - see front matter © 2009 Elsevier B.V. All rights reserved.
doi:10.1016/j.braindev.2009.05.005

1. Introduction

Autism is basically characterized by severely impaired social interaction and communication, and a limited range of activities and interests. As the diagnosis of autism is made on the basis of patients' behavioral characteristics, the disorder is not caused by only one factor. It is considered that various genetic and environmental factors are involved in the occurrence of autism, and their interactions are complex. In 1998, the International Molecular Genetic Study of Autism Consortium (IMGSC) reported their genome-wide linkage analysis of families in which there was more than one member with idiopathic autism [1]. On the basis of the results of a subsequent large-scale genome-wide scan, candidate

gene loci, including 7q21.2–q36.2, 16p12.1–p13.3, 6q14.3–q23.2, 2q24.1–q33.1, 17q11.1–q21.2, 1q21–q44, and 3q21.3–q29, were identified [2]. In an attempt to increase the linkage, a nearly homogeneous group was selected among patients with autism of heterogeneous causes. Autism patients were classified into subgroups or subsets in accordance with the phenotype of autism [3], such as through a quantitative trait locus (QTL) analysis of the constituent elements of endophenotypes in autism [4], and an ordered-subset analysis [5] was carried out. The ratio of second digit (2D) length to fourth digit (4D) length (2D/4D) is very low in some autism patients [6,7]. The *homeo box D (HOXD)* gene family is involved in skeletal morphogenesis, and correlations between digit length and the expression levels of *HOXD11*, *HOXD12*, and *HOXD13* have been observed [8,9]. In addition, *HOXD* genes form a cluster at 2q24.1–q33.1, which has been found to be a candidate locus by a genome-wide scan [3]. Therefore, we considered that digit length is one of the small physical signs of autism. Hence, we investigated the relationships between autism and polymorphism of *HOXD11*, *HOXD12*, and *HOXD13*. Moreover, we classified autism patients into two categories: patients with a low 2D/4D formed the short digit group (SDG), while the remaining patients formed the non-short-digit group (non-SDG). We also examined the genetic polymorphism of these three genes between SDG and non-SDG with autism and also between SDG with and without autism. No analysis of autism focusing on these relationships has been reported to date.

2. Subjects and methods

Seven patients with autism in the SDG were screened for the presence or absence of gene mutations in the exon and intron of *HOXD11*, *HOXD12*, and *HOXD13*, and for gene polymorphisms. The genotypic frequencies of the detected polymorphisms and the polymorphisms already listed in the GenBank were compared between the autism patients and the controls. Finally, the genotypes of the above polymorphisms of the autism patients in SDG were investigated.

2.1. Subjects

The subjects examined by genetic analysis in this study were 98 patients who visited the Department of Pediatrics, Hamamatsu University School of Medicine and Hamamatsu City Medical Center for Developmental Medicine, and who were diagnosed as having autism, PDD-NOS, and Asperger syndrome on the basis of the criteria in the Diagnostic and Statistical Manual of Mental Disorders (DSM-IV [10]). Patients with clear underlying diseases such as chromosomal abnormalities, tuberous sclerosis, and Fragile X syndrome were excluded from the study. The patients were of 82 males and 16 females with ages ranging from 5 years and 2 months to 31 years and 10 months (mean age: 12 years and 7 months). In terms of ethnicity, 95 patients had Japanese parents, 2 had Japanese fathers and Filipino mothers, and 1 had Bangladeshi parents. Eighty-nine subjects without any neurological abnormality served as healthy controls for gene analysis; all of them were Japanese and their sex and age were not determined. Thirty patients were also examined as disease controls, including 16 non-autistic patients, 14 mentally retarded patients, and 2 AD/HD patients, all of whom were Japanese.

2.2. Measurement of second and fourth digit lengths

A digital camera providing three-megapixel images was used for the measurement of the 2D and 4D lengths. Each subject's right hand was placed palm-up on a flat desk, and was photographed with the camera 20 cm above the hand. Three pediatric neurologists separately measured the 2D and 4D lengths from the line of the base to the tip of the digits three times using the image analyzing software Scion Image (NIH). The mean ratio of 2D length to 4D length (2D/4D) was calculated. In this study, patients with lower than the mean 2D/4D of the autism patients reported by Osawa et al., that is, a 2D/4D of 0.94 or lower, were classified as SDG [7].

2.3. Gene analysis

Seven patients with autism (6 males and 1 female) in the SDG were screened for the presence or absence of gene mutations and gene polymorphisms by the direct sequencing method. *HOXD11*, *HOXD12*, and *HOXD13* – each consisting of two exons and one intron – were searched for in a region from approximately 500 bp upstream, including a promoter, to approximately 500 bp downstream of the gene. Genomic DNA extracted from lymphocytes using a DNA extraction kit (Takara Co., Shiga, Japan) was used. DNA was amplified by PCR using a Taq PCR Core kit (QIAGEN Co., CA, USA), and the base sequence was obtained by the direct sequencing method. Genotypes were determined for single nucleotide polymorphism (SNP) in five loci that were newly found by this method in this study and for SNP in 20 loci that are listed in the online database GenBank (NCBL dbSNP). Genotypes in some loci were also determined by real-time PCR analysis using a TaqMan allelic discrimination assay (Applied Biosystems).

2.4. Statistical analysis

Genotypic frequency and allelic frequency of the autism patients were compared to those of the healthy con-

trol group using a χ^2 test or Fisher's exact test with SPSS 12.0J for a Windows-based System. A statistical significance level of $p \leqq 0.05$ was set.

3. Results

2D/4D was determined in 28 patients (24 males and 4 females) out of the 98 autism patients. Eleven patients (9 males and 2 females) of these 28 patients were classified as SDG. The clinical features of these patients, including sex, age, and the severity of mental retardation, are shown in Table 1. A high percentage of patients with severe mental retardation were observed in SDG with autism, whereas no patients with severe mental retardation were observed in non-SDG with autism. We also measured 2D/4D in 16 non-autistic patients in the disease control group, and 8 patients were classified as SDG and 8 patients as non-SDG. The results of the 2D/4D values of the 28 ASD and 30 non-ASD patients are shown in Fig. 1.

The results of the polymorphism analysis are shown in Table 2. No significant difference in polymorphism was observed between the autism patients and the healthy control group. However, with regarding to SNP in the promoter region of *HOXD11* G-112T, heterozygosity was observed in 4 autism patients, but not in the healthy or disease control group. The SNP in the promoter region of *HOXD12* -C226A and the SNP in

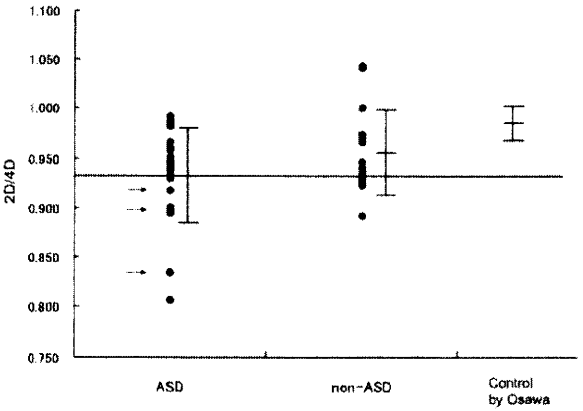

Fig. 1. 2D/4D values for the ASD28 cases and the non-ASD30 cases. Mean ± SD was presented. The M-ASD line is the average for the ASD cases; at or below this line is the SDG. As a reference, we showed the mean ± SD for normally healthy children as calculated by Osawa et al. [7]. The arrow indicates cases with *HOXD11* heterogeneity.

Table 1
Clinical features of patients.

	All the autistic disorder patients	Patients with 2D/4D determined		
		Total	SDG	NSDG
Number of patients	98	28	11	17
Sex				
Males:females	82:16 (5.1:1)	24:4 (5.5:1)	9:2 (4.5:1)	15:2 (7.5:1)
Age	5 y 2 m–31 y 10 m	5 y 4 m–31 y 10 m	8 y 1 m–31 y 10 m	5 y 4 m–16 y 7 m
Median	11 y 6 m	12 y 0 m	14 y 4 m	9 y 2 m
Mean	12 y 7 m	12 y 11 m	16 y 6 m	10 y 4 m
Family history: (3 generations)				
With[a]	22 (22.4%)	10 (35.7%)	3 (30.0%)	7 (41.2%)
Those with autism	7 (7.3%)	5 (17.9%)	2 (20.0%)	3 (17.4%)
Without	69 (70.4%)	16 (57.1%)	7 (70.0%)	7 (41.2%)
Mental retardation				
Without	10 (10.3%)	7 (25.0%)	2 (18.2%)	5 (29.4%)
Minor	21 (21.6%)	6 (21.4%)	2 (18.2%)	4 (23.5%)
Moderate	44 (45.4%)	10 (35.7%)	2 (18.2%)	8 (47.1%)
Severe	22 (22.7%)	5 (17.9%)	5 (45.5%)	0
Age at walk alone	9–48 m (91 cases)	9–48 m (26)	11–48 m (10)	9–18 m (16)
Median	13 m	12 m	12 m	12 m
Mean	13.9 m	14.3 m	18 m	12.9 m
Age at first word	10 m–6 y 10 m (80 cases)	11 m–6 y 10 m (25)	11 m–6 y 10 m (10)	1 y 3 m–3 y 5 m (15)
Median	1 y 6 m	1 y 6 m	1 y 6 m, 1 y 11 m	1 y 10 m
Mean	1 y 9 m	2 y 1 m	2 y 4 m	1 y 11 m
No. of patients 2 y or over	28	10	4	6
Age at first phrase	1 y 6 m–5 y 0 m (31 cases)	1 y 7 m–5 y 0 m (13)	2 y 6 m–5 y 0 m (5)	1 y 7 m–4 y 0 m (8)
Median	2 y 11 m	2 y 11 m	3 y 0 m	2 y
Mean	2 y 10 m	2 y 9 m	3 y 2 m	2 y 5 m
No. of patients 3 y or over	16	5	3	2

[a] Family history with psychiatric disorders including major depression, autism etc.

Table 2
Results of analysis of gene polymorphisms.

Gene	Location in gene	dtSNP ID	Allele	Frequency		Genotype	Frequency	
				Autism	Control		Autism	Control
HOXD11	Promoter		G	0.979	1	GG	0.959	1
			T	0.021	0	GT	0.042	0
						TT	0	0
	Intron	rs84746	A	0.711	0.721	AA	0.571	0.561
			C	0.289	0.288	AC	0.230	0.371
						CC	0.133	0.067
	Exon 2	rs863678	G	0.541	0.567	GG	0.316	0.292
			T	0.459	0.443	GT	0.449	0.551
						TT	0.235	0.157
	Exon2	rs6745764	A	0.214	0.18	AA	0.031	0.011
			G	0.786	0.82	AG	0.367	0.337
						GG	0.602	0.652
HOXD12	Promoter		A	0.041	0.028	AA	0	0
			C	0.959	0.972	AC	0.082	0.056
						CC	0.918	0.944
	Promoter		G	0.929	0.955	GG	0.929	0.955
			T	0.071	0.045	GT	0.071	0.045
						TT	0	0
	Exon 1	rs847151	A	0.041	0.028	AA	0	0
			G	0.959	0.972	AG	0.082	0.056
						GG	0.918	0.944
HOXD13	Promoter	rs847196	C	0.893	0.938	CC	0.786	0.876
			G	0.107	0.061	CG	0.214	0.124
						GG	0	0
	Promoter		A	0.082	0.107	AA	0	0
			T	0.918	0.893	AT	0.163	0.213
						TT	0.837	0.787
	Exon 1		C	0.985	0.989	CC	0.969	0.978
			T	0.015	0.011	CT	0.031	0.022
						TT	0	0
	Exon 1	rs2518053	A	0.408	0.455	AA	0.173	0.235
			G	0.592	0.545	AG	0.469	0.438
						GG	0.357	0.326
	Intron	rs847194	A	0.684	0.657	AA	0.459	0.404
			C	0.316	0.343	AC	0.449	0.506
						CC	0.092	0.09

SNP with no polymorphism detected in the present cases analyzed among the SNPs listed at the GenBank

HOXD11	Promoter	rs2736846	*HOXD13*	Exon 1	rs847195
	Intron	rs2736847		Exon 1	rs13392701
	Exon 2	rs12995279		Intron	rs847193
	Exon2	rs12995280		Intron	rs847192
HOXD12	Exon 1	rs2551807		Exon 2	rs28928892
	Exon2	rs2553776		Exon 2	rs28933082
				Exon 2	rs28928891

exon 1 of *HOXD12* (rs847151, G364A) showed a nearly complete linkage disequilibrium. Heterozygosity for both *HOXD12* -C226A and *HOXD12* G364A was observed in five healthy controls and eight autism patients. Furthermore, all of the five controls heterozygous for *HOXD12* -C226A and *HOXD12* G364A were homozygous for *HOXD11* -G112G. On the other hand, of the eight autism patients heterozygous for both *HOXD12* -C226A and *HOXD12* G364A, four were homozygous and four were heterozygous for *HOXD11* G-112T. Taken together, heterozygosity in all the three loci *HOXD11* G-112T, *HOXD12* -C226A, and *HOXD12* G364A was found in four autism patients but not in the healthy controls. Table 3 shows the relationships between the polymorphisms in these three loci for two cases: SDG and non-SDG with autism and SDG and non-SDG without autism. Of the four patients heterozygous for *HOXD11* G-112T, three in whom digit length was measured were classified into SDG with autism and the rest was unknown. The clinical type of ASD of the patients with having *HOXD11* heterogeneity was classified as autistic disorder in all cases. No patients

Table 3
Frequency of *HOXD* gene polymorphisms between SDG and NSDG patients with or without autism.

Gene	dbSNP ID	Genotype	Autistic patients			Normal	Non-autistic	
			Total	SDG	NSDG	Control	SDG	NSDG
HOXD11		GG	94	8	17	89	8	8
		GT	4	3	0	0	0	0
HOXD12		CC	90	8	17	84	8	8
		AC	8	3	0	5	0	0
HOXD12	rs847151	GG	90	8	17	84	8	8
		AG	8	3	0	5	0	0

heterozygous for *HOXD11* G-112T were observed among the 16 non-autistic disease controls including the eight patients with SDG.

4. Discussion

In genetic research for autism, some studies have been conducted that focused mainly on language development skills (e.g., age at first word, age at first phrase, onset of first phrase >36 months, and nonverbal communication) skill. Other studies have focused on the establishment of motor language development, bladder and bowel control milestones, developmental regression, repetitive/stereotyped behavior, restricted behavior, interest, and activity [2–4,11–13].

Manning et al. [6] reported that 2D/4D is low in autism and Asperger syndrome. In Japan, Osawa et al. [7] reported a higher incidence of low 2D/4D in autism patients than in healthy children. From their report, we assumed that it is possible to consider a low 2D/4D as a specific feature in some autism patients. Such patients formed part of a group of subjects (SDG) for investigation in our study. It was assumed that SDG in autism may express one of the common features; hence, 2D/4D may be associated with one of the etiological genes of autism. Manning et al. [14] reported the findings of their 2D/4D measurement as follows: (1) there is a gender difference in 2D/4D measurements (2D/4D is lower in males than in females); (2) a low 2D/4D is observed across races and countries; (3) 2D/4D is closely related to fetal growth, sperm count, family size, myocardial infarction, and breast cancer; and (4) 2D/4D is related to sexual differentiation, the production of sex hormones in the fetal stage, and disease programming in the fetal stage. In addition, there is an inverse correlation between 2D/4D and testosterone concentration at the fetal stage, and 2D/4D correlates with the CAG repeat number in the androgen receptor gene [15].

A study of female twins conducted by Paul et al. [16] showed that the concordance rate of 2D/4D is higher in monozygotic twins than in dizygotic twins, that the heritability of 2D/4D is approximately 66%, and that the genetic contribution to 2D/4D in females may be more influential than the effects of prenatal environmental factors. Although it is uncertain whether these findings differ significantly between males and females in the absence of any report for males, it seems possible that 2D/4D is affected by both hereditary and secondary perinatal environmental factors.

One study showed that the mean 2D/4D did not change with gestational age from the 9th week to the 40th week [17]. In addition, there was a small increase in 2D/4D with age, which was lowest in the right hand [18]. This study indicates that 2D/4D is probably established in the uterus and that this ratio remains almost constant until adult life.

Because 2D/4D, an easily measurable physical feature, is already determined in utero and remains constant until adult life, it can be used regardless of age differences among subjects and is universal; moreover, its measurement is noninvasive. Therefore, 2D/4D is an excellent parameter for evaluating a group of autistic patients.

In genomic scans of families having more than one member with autism, the susceptibility loci for autism were investigated, and identified; these included 2q21–q33 [3,4]. In the candidate genes located here, the NRP2 gene is reported as one of the genes related to autism [19]. In addition, specific polymorphism has been found in distal-less 2 (DLX2) and cAMP guanine nucleotide exchange factor II (cAMP-GEFII) in a few cases of autism [20]. On the other hand, no significant correlation has been reported between autism and distal-less 1 (DLX1) [20,21] and DLX2 [20]. With regard to *HOXD* genes, Bacchlli et al. reported that there is no relationship between *HOXD1* and autism [20]. There has been no report on *HOXD11*, *HOXD12* or *HOXD13* to date.

It seems that these genes may be found to be significant in the development of autism when cases as a study subject have been carefully chosen and classified by the specific characteristics of presenting behavior or phenotypic clinical presentations.

The present study has limitations because it is a case-control study, rather than a family study, with a small number of subjects enrolled. However, in this study,

HOXD11 SNP -112G/-112T heterozygosity was specifically observed in autism patients with low 2D/4D. On the basis of this result, we expect that the relationships between autism and the *HOXD* genes or other candidate genes located in 2q will be clarified by studying a larger population with low 2D/4D, that is, by studying patients heterozygous for -112G/-112T in the *HOXD11* promoter.

References

[1] International Molecular Genetic Study of Autism Consortium. A full genome screen for autism with evidence for linkage to a region on chromosome 7q. Hum Mol Genet 1998;7:571–8.

[2] Yang MS, Gill M. A review of gene linkage, association and expression studies in autism and an assessment of convergent evidence. Int J Dev Neurosci 2007;25:69–85.

[3] Buxbaum JD, Silverman JM, Smith CJ, Kilifarski M, Reichert J, Hollander E, et al. Evidence for a susceptibility gene for autism on chromosome 2 and for genetic heterogeneity. Am J Hum Genet 2001;68:1514–20.

[4] Shao Y, Wolpert CM, Raiford KL, Menold MM, Donnelly SL, Ravan SA, et al. Genomic screen and follow-up analysis for autistic disorder. Am J Med Genet 2002;114:99–105.

[5] Alarcón M, Cantor RM, Liu J, Gilliam Cthe Autism Genetic Resource Exchange Consortium, Geschwind H. Evidence for a language quantitative trait locus on chromosome 7q in multiplex autism families. Am J Med Genet 2002;70:60–71.

[6] Manning JT, Baron-Cohen S, Wheelwright S, Sanders G. The 2nd to 4th digit ratio and autism. Dev Med Child Neurol 2001;43:160–4.

[7] Osawa J, Sugie H, Fukuda T, Ito M, Sugie Y, Ohzeki T. Evaluation of the 2nd to 4th digit ratio in the patients with autism. No To Hattatsu (Tokyo) 2005;37:424–5, [in Japanese].

[8] Zákány J, Fromental-Ramain C, Warot X, Duboule D. Regulation of number and size of digits by posterior Hox genes: a dose-dependent mechanism with potential evolutionary implications. Proc Natl Acad Sci USA 1997;94:13695–700.

[9] Kuroiwa A. The role of homeobox genes on cartilage pattern formation. Jikken Igaku 2002;17:2441–8, [in Japanese].

[10] American Psychiatric Association. Diagnostic and statistical manual of mental disorders. 4th ed. Washington, DC: American Psychiatric Association; 1994.

[11] Alarcón M, Yonan AL, Gilliam TC, Cantor RM, Geschwind DH. Quantitative genome scan and Ordered-Subsets Analysis of autism endophenotypes support language QTLs. Mol Psychiatry 2005;10:747–57.

[12] Freitag CM. The genetics of autistic disorders and its clinical relevance: a review of the literature. Mol Psychiatry 2007;12:2–22.

[13] Alarcón M, Abrahams BS, Stone JL, Duvall JA, Perederiy JV, Bomar JM, et al. Linkage, association, and gene-expression analyses identify *CNTNAP2* as an autism-susceptibility gene. Am J Hum Genet 2008;82:150–9.

[14] Manning JT, Churchill AJ, Peters M. The effects of sex, ethnicity, and sexual orientation on self-measured digit ratio (2D:4D). Arch Sex Behav 2007;36:223–33.

[15] Manning JT, Bundred PE, Flanagan BF. The ratio of 2nd to 4th digit length: a proxy for transactivation activity of the androgen receptor gene? Med Hypotheses 2002;59:334–6.

[16] Paul SN, Kato BS, Cherkas LF, Andrew T, Spector TD. Heritability of the second to fourth digit ratio (2d:4d): a twin study. Twin Res Hum Genet 2006;9:215–9.

[17] Malas MA, Dogan S, Evcil EH, Desdicioglu K. Fetal development of the hand, digits and digit ratio (2D:4D). Early Hum Dev 2006;82:469–75.

[18] Trivers R, Manning J, Jacobson AA. Longitudinal study of digit ratio (2D:4D) and other finger ratios in Jamaican children. Horm Behav 2006;49:150–6.

[19] Wu S, Yue W, Jia M, Ruan Y, Lu T, Gong X, et al. Association of the neuropilin-2 (NRP2) gene polymorphisms with autism in Chinese Han population. Am J Med Genet B Neuropsychiatr Genet 2007;144B:492–5.

[20] Bacchelli E, Blasi F, Biondolillo M, Lamb JA, Bonora E, Barnby G, et al. Screening of nine candidate genes for autism on chromosome 2q reveals rare nonsynonymous variants in the cAMP-GEFII gene. Mol Psychiatry 2003;8:916–24.

[21] Hamilton SP, Woo JM, Carlson EJ, Ghanem N, Ekker M, Rubenstein JL. Analysis of four DLX homeobox genes in autistic probands. BMC Genet 2005;6:52.

of p62 positive aggregates correlate pretty well with myofiber atrophy. In general the degradation systems appear to be still functioning in these patients and seem to contribute positively to counteract disease progression. In conclusion, present data underline the role of unproductive autophagy and accumulation of aggregate-prone ubiquitinated proteins in the pathogenesis of GSDII, especially in more severely affected patients.

SM202. An exploratory analysis of scoliosis in 182 children and adults with Pompe disease from the Pompe Registry

Merlini, Luciano[1]; Case, Laura[2]; Kishnani, Priya[2]; Muller-Felber, Wolfgang[3]; Roberts, Mark[4]; van der Ploeg, Ans[5]; Prasad, Suyash[6]

[1]University of Ferrara, Ferrara, Italy; [2]Duke University Medical Center, Durham, United States; [3]Friedrich-Baur Institute, Munich, Germany; [4]Withington Hospital, Manchester, United Kingdom; [5]Erasmus Medical Center, Rotterdam, Netherlands; [6]Genzyme Corporation, Cambridge, United States

The prevalence of scoliosis and its relationship with respiratory function are explored in patients enrolled in the Pompe Registry. Scoliosis status was reported for 575 patients, 182 of whom had scoliosis (25 children age 0 to < 2 years or ≥ 2 to < 13 years; 24 teenagers age ≥ 13 to < 20 years, and 133 adults age ≥ 20 years).

Children age ≥ 2 years with scoliosis had a mean age at Pompe symptom onset of 1.1 years, identical to children without scoliosis. Teenagers with scoliosis had a mean age at symptom onset of 5.8 years compared with 9.1 years in teenagers without scoliosis. Adults with scoliosis had mean age at symptom onset of 25.3 years compared with 32.8 years in adults without scoliosis.

Among the subset of patients with FVC data, children age ≥ 2 years (n = 6) and teenagers (n = 9) with scoliosis had lower % predicted forced vital capacity (FVC) upright median scores (68.0% and 59.0%, respectively) than those in similar age groups without scoliosis (15 children, 5 teenagers; 77.0% and 91.1%, respectively). Children age ≥ 2 years with scoliosis (n = 3) had lower median % predicted FVC supine scores than those in similar age groups without scoliosis (n = 5) (47.0% versus 70.0%, respectively). Supine scores for teenagers without scoliosis were unavailable. Among adults, FVC % predicted upright and supine median scores were similar regardless of scoliosis status.

Further analysis and collection of detailed scoliosis and respiratory function data is needed to better understand this relationship and how scoliosis affects quality of life in patients with Pompe disease.

SM203. Quantitative metabolome profiling of biopsied muscle in the patients with glycogen storage diseases using capillary electrophoresis mass spectrometry

Fukuda, Tokiko[1]; Sugie, Yoko[2]; Sugie, Hideo[3]

[1]Jichi Medical University, Tochigi, Japan; [2]Hamamatsu Medical University, Pediatrics, Hamamatsu, Japan; [3]Jichi Medical University, Pediatrics, Shimotsuke, Japan

Metabolome analysis has lately been applied for the characterization of disease-specific metabolism. Recently developed capillary electrophoresis time-of-flight mass spectrometry (CE-TOFMS) has enabled quantitative analysis of charged metabolites by the simultaneous measurement of their levels in tissues. In order to characterize the metabolism of muscular glycogen storage diseases (M-GSD), and also to evaluate whether CE-TOFMS could be a valuable diagnostic tool for M-GSD, we applied CE-TOFMS to measure the metabolites involved in energy production in the muscles of M-GSD. Biopsied muscles were obtained from each patient with GSDIIa, IIb, III, V, VII, and phosphoglycerate kinase (PGK) deficiency. Histologically normal muscles from three myopathy patients with normal CK values were used as controls. We identified 10 metabolites involved in glycolysis, 8 in TCA cycle, and 4 in pentose phosphatase pathway. The amounts of glycolytic intermediates locating downstream of G-1-P in the glycolytic pathway were much less in muscles of GSD III and V than in control muscles, while the amounts of glycolytic intermediates locating upstream of FDP (G-6-P, G-1-P and F-6-P) and those locating upstream of 3-phosphoglycerate were significantly high in muscles of GSD VII and in PGK deficiency, respectively. There was no difference in the amounts of glycolytic intermediates between GSD II and controls. The amounts of the metabolites in TCA cycle were higher in muscles of GSD II than in controls. The metabolome analysis of biopsied muscles had clearly determined the blockage of the metabolic pathway. We conclude that this method could be a high through-put and good method for diagnosis in M-GSD.

SM204. Adult Pompe disease: bone mineral density before and after enzyme replacement therapy

Papadimas, George-Konstantinos[1]; Terzis, Gerasimos[2]; Methenitis, Spyridon[2]; Spengos, Konstantinos[2]; Papadopoulos, Constantinos[2]; Kavouras, Stavros[2]; Michelakakis, Helen[3]; Manta, Panagiota[2]

[1]University of Athens, Medical School, Neurology, Athens, Greece; [2]University of Athens, Athens, Greece; [3]'Ag. Sophia' Children's Hospital, Athens, Greece

Pompe disease is an autosomal recessive disorder caused by lysosomal α-glycosidase deficiency. The infantile form is characterized by cardiomegaly and severe muscle weakness with an early fatal outcome, while the adult form is usually milder with progressive muscle weakness and respiratory dysfunction. Bone mineral density (BMD) seems to be decreased in the infantile form leading to osteopenia and fractures, but data concerning the adult form of the disease are still limited. The aim of the present study is to evaluate BMD in patients with the adult form of Pompe disease before and after enzyme replacement therapy (ERT).

Body composition was examined by means of dual x-ray absorptiometry at baseline and after 9-12 months of ERT in five patients with the adult onset form of Pompe disease.

One patient had reduced BMD in total body, L2-L4 spine and femoral neck in the range of osteopenia, one other had reduced L2-L4 spine BMD and two patients had slightly reduced femoral neck BMD. After 9-12 months of ERT, BMD was not considerably altered in any patient.

A slight reduction of BMD among patients with the adult form of Pompe disease might be occasionally found. The short-

Journal of Human Genetics (2010) 55, 590–599

www.nature.com/jhg

ORIGINAL ARTICLE

Copy-number variations on the X chromosome in Japanese patients with mental retardation detected by array-based comparative genomic hybridization analysis

Shozo Honda[1], Shin Hayashi[1], Issei Imoto[1,2], Jun Toyama[3], Hitoshi Okazawa[4], Eiji Nakagawa[5,6], Yu-ichi Goto[5,6] and Johji Inazawa[1,2,7], Japanese Mental Retardation Consortium[8]

X-linked mental retardation (XLMR) is a common, clinically complex and genetically heterogeneous disease arising from many mutations along the X chromosome. Although research during the past decade has identified >90 XLMR genes, many more remain uncharacterized. In this study, copy-number variations (CNVs) were screened in individuals with MR from 144 families by array-based comparative genomic hybridization (aCGH) using a bacterial artificial chromosome-based X-tiling array. Candidate pathogenic CNVs (pCNVs) were detected in 10 families (6.9%). Five of the families had pCNVs involving known XLMR genes, duplication of Xq28 containing *MECP2* in three families, duplication of Xp11.22-p11.23 containing *FTSJ1* and *PQBP1* in one family, and deletion of Xp11.22 bearing *SHROOM4* in one family. New candidate pCNVs were detected in five families as follows: identical complex pCNVs involved in dup(X)(p22.2) and dup(X)(p21.3) containing part of *REPS2*, *NHS* and *IL1RAPL1* in two unrelated families, duplication of Xp22.2 including part of *FRMPD4*, duplication of Xq21.1 including *HDX* and deletion of Xq24 noncoding region in one family, respectively. Both parents and only mother samples were available in six and three families, respectively, and pCNVs were inherited from each of their mothers in those families other than a family of the proband with deletion of *SHROOM4*. This study should help to identify the novel XLMR genes and mechanisms leading to MR and reveal the clinical conditions and genomic background of XLMR.
Journal of Human Genetics (2010) **55**, 590–599; doi:10.1038/jhg.2010.74; published online 8 July 2010

Keywords: array CGH; *FRMPD4*; *HDX*; *MECP2*; pCNV; *PQBP1*; *SHROOM4*; XLMR

INTRODUCTION

Mental retardation (MR) is characterized by nonprogressive cognitive impairment and affects 1–3% of the general population. The predominance of males in the MR population has been attributed to genes located on the X chromosome. In fact, individual X-linked genes were recently estimated to contribute to 10–12% of all MR cases in males.[1] X-linked MR (XLMR) conditions have been divided into syndromic (MRXS representing approximately one-third of XLMR) and nonsyndromic (MRX representing approximately two-third of XLMR).[2] As MRX have no obvious and consistent phenotypes other than MR, XLMR conditions are clinically diverse and genetically heterogeneous disorders. In excess of 215 XLMR conditions have been recorded (http://xlmr.interfree.it/home.htm and http://www.ggc.org/xlmr.htm) and 90 XLMR genes have been identified.[3,4] Genes for 87 conditions have been mapped by linkage analysis and/or cytogenetic breakpoints, but for 38 conditions, genes have been neither identified nor mapped to candidate loci. In addition, more than 300 X-linked protein-coding genes are expressed in brain tissue, suggesting that many XLMR genes remain to be unidentified.[5]

[1]Department of Molecular Cytogenetics, Medical Research Institute and School of Biomedical Science, Tokyo Medical and Dental University, Tokyo, Japan; [2]Hard Tissue Genome Research Center, Tokyo Medical and Dental University, Tokyo, Japan; [3]Department of Pediatrics, Okinawa Child Development Center, Okinawa, Japan; [4]Department of Neuropathology, Medical Research Institute and School of Biomedical Science, Tokyo Medical and Dental University, Tokyo, Japan; [5]Department of Child Neurology, National Center Hospital, National Center of Neurology and Psychiatry (NCNP), Tokyo, Japan; [6]Department of Mental Retardation and Birth Defect Research, National Institute of Neuroscience, NCNP, Tokyo, Japan and [7]Grobal Center of Excellence Program for Frontier Research on Molecular Destruction and Reconstitution of Tooth and Bone, Tokyo Medical and Dental University, Tokyo, Japan
[8]See Appendix.
Correspondence: Professor J Inazawa, Department of Molecular Cytogenetics, Medical Research Institute, Tokyo Medical and Dental University, 1-5-45 Yushima Bunkyo-ku, Tokyo 113-8510, Japan.
E-mail: johinaz.cgen@mri.tmd.ac.jp
This work is part of an ongoing study by the Japanese Mental Retardation Research Consortium.
Received 19 March 2010; revised 19 May 2010; accepted 26 May 2010; published online 8 July 2010

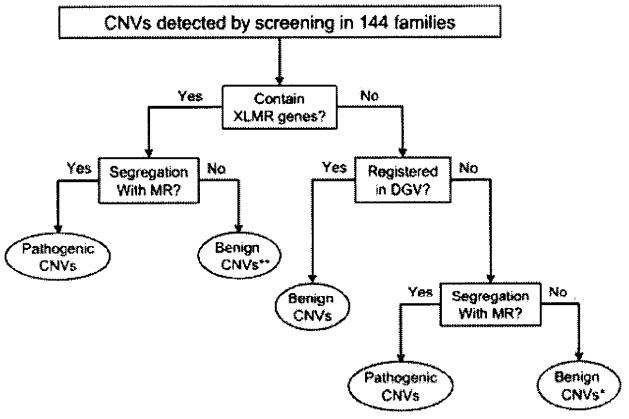

Figure 1 The flowchart of the screening of MR-associated pathogenic CNV. DGV means database of genomic variants. Asterisks indicate types of benign CNVs corresponding to asterisks in Supplementary Table S1.

Array-based comparative genomic hybridization (aCGH) has revealed copy-number variations (CNVs) to be the cause of MR.[6–8] Although Tarpey *et al.*[4] screened for mutations in the coding regions of 718 genes on the X chromosome in probands from 208 families by means of resequencing, only three XLMR-associated genes have been identified, suggesting structural variations other than point mutations, including CNVs or variants in regulatory regions, to contribute to unidentified XLMR conditions.

In this study, we examined CNVs in individuals with MR from 144 families with at least one affected male by aCGH using an in-house bacterial artificial chromosome (BAC)-based X-tiling array (MCG X-tiling array).[9] We detected 10 candidate pathogenic CNVs (pCNVs) according to a flowchart of our procedure (Figure 1), suggesting that pCNVs on the X chromosome could be found at a constant rate by the high-density aCGH in heterogeneous MR patients and our approach is useful to identify known as well as novel XLMR genes, resulting in a better understanding of the clinical conditions and genetic background of XLMR, although further study is needed to assess the significance of candidate XLMR-related genes.

MATERIALS AND METHODS

Patients

We selected 144 families with at least one male having MR. 'Familial type' MR, that is more than two members of the family affected, was identified in 76 families and 'sporadic type' MR, that is only one male affected, was found in 68 families. The male probands were subjected to an aCGH using the MCG X-tiling array.[9] In 131/144 cases, conventional karyotyping was performed, and an abnormal karyotype of 46,XY,der(18)t(5;18)(p13;p11.3)pat(20/20) was detected in one case.

Cell culture

Peripheral blood samples were obtained with informed consent approved by the Institutional Review Board, National Center of Neurology and Psychiatry, Japan. Epstein–Barr virus-transformed lymphoblast cell lines (LCLs) were established from peripheral blood cells. All LCLs were cultured in RPMI1640 medium supplemented with 10% fetal bovine serum and antibiotics.

aCGH using an in-house BAC array

aCGH hybridization using the MCG X-tiling array was performed as described previously with DNA extracted from sex-matched normal lymphocytes as a reference.[10] Acquired images from hybridized slides were analyzed with GenePix Pro 6.0 (Axon Instruments, Foster City, CA, USA). Fluorescence ratios were normalized so that the mean of the middle third of $\log_2$ ratio across the array was zero. The thresholds for copy-number gain and loss were set at log2 ratios of 0.4 and −0.4, respectively.

High-density oligonucleotide aCGH

A genome-wide oligonucleotide aCGH was performed using 244K (Agilent Technologies, Santa Clara, CA, USA) according to the directions provided by the manufacturer. The hybridized arrays were scanned using an Agilent scanner, and the CGH Analytics program version 3.4.40 (Agilent Technologies) was used to analyze copy-number alterations after data extraction, filtering and normalization by Feature Extraction software (Agilent Technologies).

FISH

Metaphase chromosomes were prepared from normal peripheral lymphocytes and from each of the LCLs in all family members using the standard method. Fluorescent *in situ* hybridization (FISH) analyses were performed as previously described,[10] using BAC clones located around the region of interest as probes.

Quantitative real-time reverse transcriptase-PCR

cDNAs were synthesized from total RNA extracted from LCLs established from the patients, their parents and six normal controls (three males and three females). Quantitative real-time reverse transcriptase PCR was performed with the ABI PRISM 7500 sequence detection System (Applied Biosystems, Foster City, CA, USA) using TaqMan Gene Expression Assays (Hs00202185_A1 FTSJ1, Hs00172868_A1 PQBP1, Applied Biosystems) according to the manufacturer's instructions. mRNA levels of the genes of interest were normalized against a housekeeping gene, *GAPDH* (Hs9999905_A1 GAPDH, Applied Biosystems), as an internal control to collect the relative expression data. Each assay was performed in triplicate for each sample.

The *androgen receptor* X-inactivation assay and late replication assay

The pattern of X-chromosome inactivation in the females was first evaluated using the *androgen receptor* X-inactivation assay[11] with minor modifications. Briefly, DNA was modified with sodium bisulfite and amplified with primers specific for a methylated or unmethylated DNA sequence at the human *androgen receptor* locus where methylation correlates with X-inactivation. Two different sized products, which were gained from the paternal and maternal alleles because of the polymorphism of the triplet repeat, were analyzed on a 3130 Genetic Analyzer (Applied Biosystems), and peak images of each PCR product were measured by GeneMapper Software v4.0 (Applied Biosystems). An imbalance of X-chromosome inactivation (skewing) was judged from the ratio between the amount of PCR product from paternal and maternal alleles. These ratios were corrected using a calculation previously described.[11]

A late replication assay was performed using a replication G-banding technique as previously reported[12] with minor modifications. Metaphase chromosomes were prepared with adjunction of 5-bromo-2-deoxiuridine in the last 6 h of cell culture after thymidine synchronization. The chromosome slides were stained with Hoechst 33258 (1 mg ml^{-1}) (Sigma, Saint Louis, MO, USA) for 5 min, and exposed to 254-nm ultraviolet light (Stratalinker UV Crosslinker 1800; Agilent Technologies) at a distance of 20 cm for 10 min after heating at 75 °C for 10 min. These chromosomes were used for FISH to estimate the ratio of inactivation of the affected X chromosome.

RESULTS

Classification of CNVs

We screened CNVs on the X chromosome in probands of 144 families with at least one affected male, by array CGH using the MCG X-tiling array to identify novel XLMR-related genes. We designed a flowchart for the classification of CNVs (Figure 1). If we detected a CNV containing known XLMR-related genes or of unknown biological or clinicopathological significance (National Center for Biotechnology

Information, http://www.ncbi.nlm.nih.gov/) and not registered in the Database of Genomic Variants (DGVs, http://projects.tcag.ca/variation/) in the male proband, we examined other family members using FISH. If the same CNV was segregated into cases of MR in the same family, it was considered a candidate for a pCNV, although CNVs observed in unaffected females in the same family or sporadic type were not excluded. Consistent with previous reports (5/108=4.6%[13] or 8/54=14.8%[14]), putative MR-associated pCNVs were detected in 10 families (6.9%, Table 1; Figure 2). The CNVs detected in five families contained known XLMR genes, whereas five candidate pCNVs seemed to be novel, although their pathogenic significance will need to be determined. The detection rates for the 'familial type' and 'sporadic type' were 7.9% (6/76) and 5.9% (4/68), respectively, suggesting that we cannot ignore the 'sporadic type' in the screening of candidate pCNVs. Each of pCNVs detected in 9 of 10 families was inherited from probands' mothers, respectively, suggesting that those CNVs were not altered through the establishment of each of the Epstein–Barr virus-transformed LCLs. In these 10 families, no abnormality was detected by conventional cytogenetics. In addition, no CNV possibly related to MR was detected in autosomes with the high-density oligonuculeotide array. Family trees of the 10 families are presented in Figure 3.

Frequent duplication at Xq28 including *MECP2*

Duplications at Xq28 including *MECP2* (OMIM 300005) were observed in 3 of 144 families (2.1%; MRYB6, MR1P3 and MR347 families in Table 1). These patients had several common phenotypes, such as severe MR, muscular hypotonia, absence of speech and recurrent respiratory infections as reported,[15–19] although the size of genes within the affected regions differed among the three families (Supplementary Figure S4a). The smallest region of overlap was ~437 kb and contained 13 genes including *L1CAM* (OMIM 08840) and *MECP2*. FISH using an *MECP2*-specific probe revealed that the mothers in all three families were carriers (Supplementary Figures S1a, S1b and S1c) and had a skewed X-inactivation pattern (Table 1) and dominant late replication pattern of the *MECP2*-duplicated allele (data not shown). In patients and the mother of family MR347, an ~182-kb deletion at Xp22.31, which contains no protein-coding gene (Supplementary Figure S4b), was detected simultaneously by aCGH analyses using an X-tilling array and Agilent oligonucleotide array, suggesting this CNV to be of unknown biological or clinical pathological significance. In addition, the CNVs at autosomal region not registered in the DGV were detected in each of the probands in three families. (Supplementary Table S2) According to ISCN 2009,[20] these CNVs are as follows: MRYB6 had arr 15q21.2 (50 711 956–50 777 075)×1; MR1P3 had arr 20p13(897 451–956 849)×1; MR347 had arr 4q13.1(61 867 547–61 924 356)×1 and arr 15q23(65 693 871–65 713 056)×1.

Aberrations at Xp11.22-p11.23 detected in two families contain known MR-related genes

We detected candidate pCNVs at Xp11.22-p11.23 in 2 of 144 families (1.4%; MR67H and MRF91 in Table 1), although the affected regions showed no overlap between these two families (Figure 4).

MRF91

The male proband (III-1) of family MRF91 showed moderate MR and speech delay. In this patient, an ~1.37-Mb duplication at Xp11.23 was detected (Figure 2). Information from the UCSC genome browser (http://genome.ucsc.edu/cgi-bin/hgGateway) revealed that the duplicated region is gene-dense, and includes three known MR-related genes, *FTSJ1* (OMIM 300499), *PQBP1* (OMIM 300463) and *SYP* (OMIM 313475). No mutation was detected in those genes in the proband (data not shown). FISH revealed the duplication in the proband (III-1), mother (II-2) and his affected younger sister (III-2) (Supplementary Figure S1d). The mRNA levels of *FTSJ1* and *PQBP1* in LCLs determined by quantitative real-time reverse transcriptase-PCR were highest in the proband (Supplementary Figure S2). *SYP* mRNA levels could not be evaluated due to low expression in LCL. The X-chromosome inactivation in LCL showed a skewed pattern in the unaffected mother and random pattern in the affected sister (Supplementary Figure S3a). In addition, dup(X)(p11.23) showed a late replicating pattern in 39/50 cells (78%) of the unaffected mother and 24/50 cells (48%) of the affected sister (Supplementary Figure S3b). The high-density oligonucleotide aCGH revealed that the duplication at Xp11.23 in family MRF91 was flanked distally by a segmental duplication containing a synovial sarcoma X breakpoint families (*SSX1*, *SSX9*, *SSX4*, *SSX3* and *SSX4B*) and proximally by an additional segmental duplication containing G-antigen (*GAGE*) families (Figure 4). The aberration is as follows: arr Xp11.23 (48 089 045–49 246 795)×2 mat.

MR67H

The male proband of family MR67H showed only moderate MR. In this patient (III-1), an ~2.86-Mb deletion at Xp11.22, which has never been reported, was detected (Figure 2). Information from the UCSC genome browser revealed that the deleted region contains *SHROOM4* (OMIM 300579), reported to be a causative gene for XLMR.[21] Sample of his mother (II-4) was not available. The high-density oligonucleotide aCGH revealed that the deletion at Xp11.22 in family MR67H was also flanked distally by a sequence gap and proximally by a complex repeat-rich locus containing *SSX* families (*SSX7* and *SSX2*), *melanoma antigen* (*MAGE*) families and *X-antigen* (*XAGE*) families (Figure 4). The aberration is as follows: arr Xp11.22 (50 040 995–52 710 691)×0.

Other novel candidate pCNVs in five families

Identical complex pCNVs detected in nonconsanguineous MR22T and MRK13 families. The proband (III-1) of MR22T was diagnosed with West syndrome from electroencephalogram and showed severe MR, epilepsy, absence of speech and atrophy of the hippocampus, whereas patients (II-1, II-2) of family MRK13 manifested moderate MR, speech delay and autistic feature. Although the MR22T and MRK13 families are not consanguineous, identical duplications at the same two loci were detected: dup(X)(p22.2) containing part of *NHS* (OMIM 300457) and part of *REPS2* (OMIM 300317), and dup(X)(p21.3) containing part of *IL1RAPL1* (OMIM 300206), which was identified as an XLMR-related gene (OMIM 300143) (Supplementary Figures S4c and d). The aberration is as follows: arr Xp22.2 (16 898 131–17 635 375)×2 mat and arr Xp21.3 (28 711 594–28 812 042)×2 mat. The X-chromosome inactivation of mothers in both families showed a skewed pattern (Table 1). FISH analysis revealed that the signal for a BAC RP11-438J7 at Xp21.3 appeared separately at Xp21.3 and Xp22.2 and the signal at Xp22.2 could be detected more strongly (Figure 5).

MR1WK

The male proband (II-2) of family MR1WK showed mild MR and autism. An ~0.57-Mb duplication at Xp22.2 including a part of *FRMPD4* was detected in the patient. The high-density oligonucleotide aCGH revealed that the duplication also includes *MSL3* distal to *FRMPD4* (Supplementary Figure S4e). The aberration is as

Table 1 Summary of 10 families detected MR-associated pathogenic CNVs by array CGH analyses

Family	Family type	Locus	Aberr	BAC-based X-tiling array Start BAC	BAC-based X-tiling array End BAC	Size (Mb)	Genes	Candidate genes	Inheritance	Segregation	X-inactibvation	Phenotypes of patients
				Agilent 244K Start (bp)	Agilent 244K End (bp)	Size (bp)						
Known XLMR genes												
MRYB6	F	Xq28	Dup	RP11-846A22	CTC-384K8	0.59	22	*MECP2*	Inherited	Yes	m:80/20	Severe MR, muscular hypotonia, absent speech, reccurent respiratory infection
				152,721,477	153,436,833	715,357	31					
MR1P3	S	Xq28	Dup	RP11-846A22	RP11-119A22	0.33	10	*MECP2*	Inherited	Yes	m:70/30	Severe MR, muscular hypotonia, absent speech, reccurent respiratory infection
				152,676,750	153,158,866	482,117	19					
MR347	F	Xp22.31	Del	RP11-280C22	RP11-10G18	0.28	1	*NLGN4*	Inherited	Yes	m:96/4	Severe MR, muscular hypotonia, absent speech, reccurent respiratory infection, strong autistic feature
				6,213,159	6,395,371	182,213	0					
		Xq28	Dup	RP11-846A22	RP11-119A22	0.33	10	*MECP2*	Inherited	Yes		
				152,721,477	153,266,394	544,918	18					
MR67H	F	Xp11.22	Del	RP11-805H4	RP11-155M8	2.86	17>	*SHROOM4*	NA	NA	NA	Moderate MR
				50,040,995	52,710,691	2,669,697	>15					
MRF91	F	Xp11.23	Dup	RP11-344N17	RP11-211H10	1.37	39>	*FTSJ1, PQBP1, SYP*	Inherited	Yes	m:54/46 as:82:18	Moderate MR, speech delay
				48,089,045	49,246,795	1,157,751	>38					
Novel pCNV												
MR22T	S	Xp22.2	Dup	RP11-2K15	RP11-115I10	0.69	2	*REPS2, NHS*	Inherited	Yes	m:86/14	West syndrpme, severe MR, epilepsy, absent speech, artrophy of the hippocampus
				16,898,131	17,635,375	737,245	2					
		Xp21.3	Dup	RP11-639G8	RP11-438J7	0.23	1	*IL1RAPL1*	Inherited	Yes		
				28,711,594	28,812,042	100,449	1					
MRK13	S	Xp22.2	Dup	RP11-2K15	RP11-115I10	0.69	2	*REPS2, NHS*	Inherited	Yes	m:98/2	Moderate MR, speech delay, autistic feature
				16,898,131	17,635,375	737,245	2					
		Xp21.3	Dup	RP11-639G8	RP11-438J7	0.23	1	*IL1RAPL1*				
				28,711,594	28,812,042	100,449	1					
MR1WK	S	Xp22.2	Dup	RP11-797I1	RP11-937L19	0.57	1	*FRMPD4*	Inherited	Yes	m:59/41	Mild MR, autism
				11,680,788	12,313,191	632,404	2					
MR494	F	Xq21.1	Dup	RP11-74B21	RP11-405O21	0.33	1	*HDX*	Inherited	Yes	m:60/40 as:92:8 sb:96:4	Border-mild MR, epilepsy
				83,463,344	84,006,214	542,871	1					
MR86B	F	Xq24	Del	RP11-566B18	RP11-94I22	0.18	0	ND	Inherited	Yes	m:83/17	Moderate MR
				120,358,756	120,574,498	215,742	0					

F, familial type; S,sporadic type; Aberr, aberration; Dup, duplication; Del, deletion; NA, not available; ND, not determined.
m, X-inactivation pattern from the carrier mother; as, affected sister; sb, sister showing border of MR.

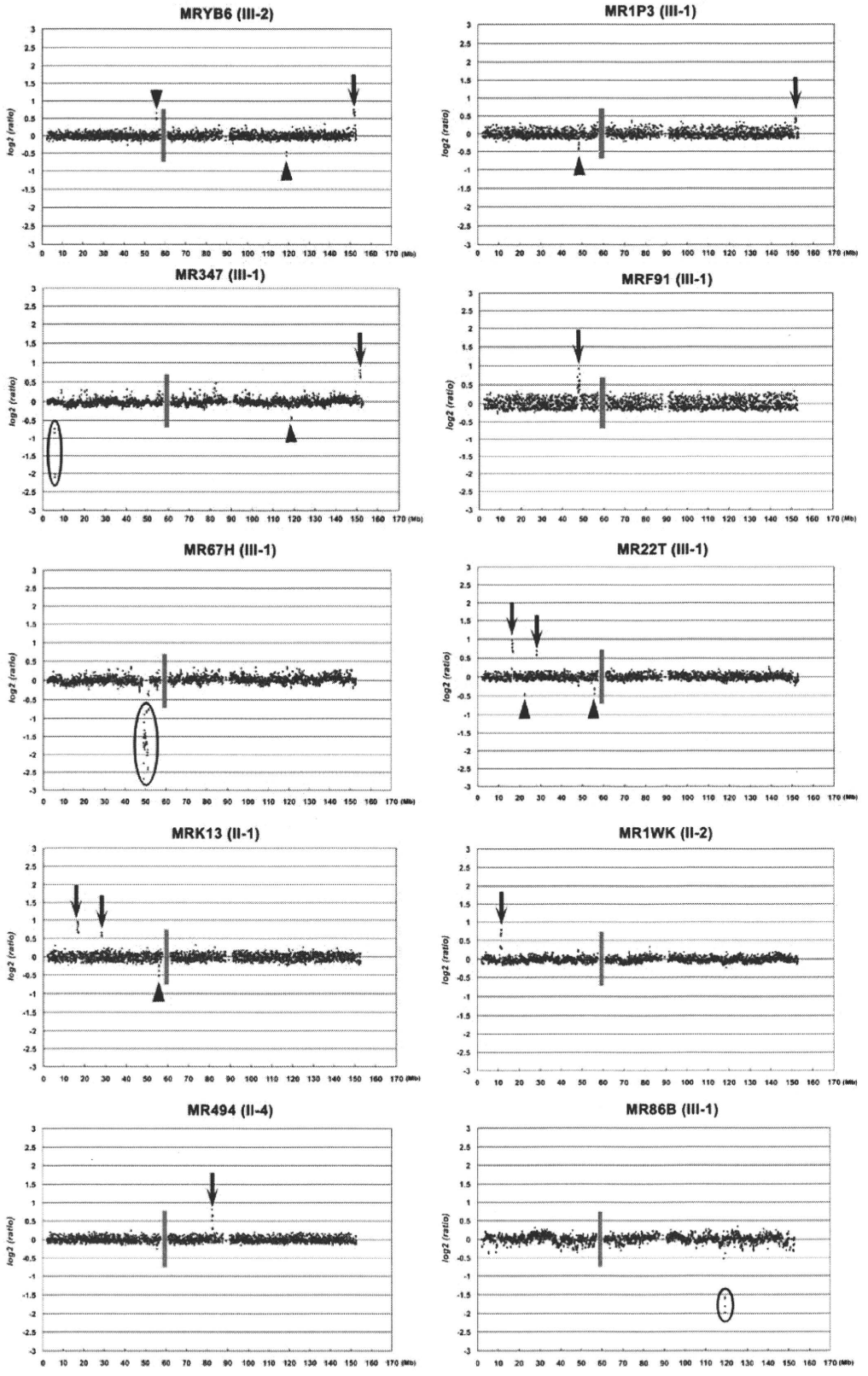

Figure 2 Results of array-CGH analysis with the X-tiling array in probands of 10 families in which candidate pCNVs were detected. Each dot represents the log2 ratio of a BAC, and arrows and circles indicate MR-associated duplications (ratio >0.4) and homozygous deletions (ratio <-0.7), respectively. Arrowheads indicate benign CNVs. The gray vertical lines represent the centromeric region for which no clones were available.

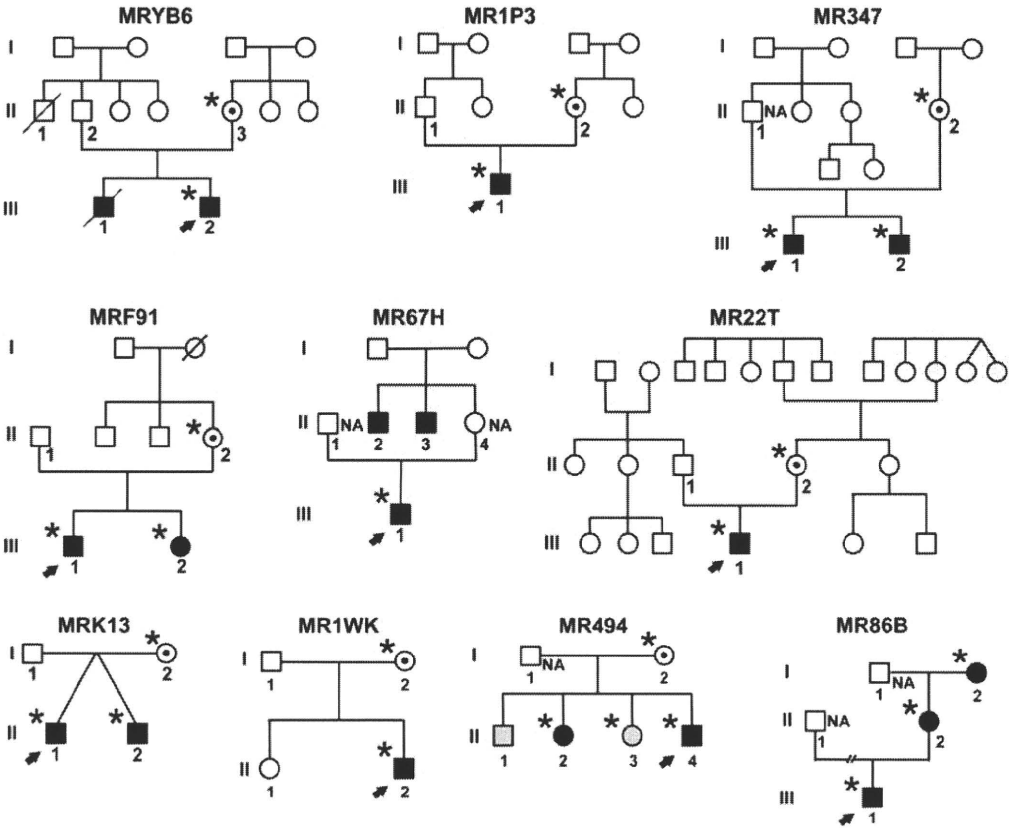

Figure 3 Pedigrees of 10 families in which probable pCNVs were detected. Closed squares and circles, gray squares and circles, and dotted circles indicate MR, borderline MR and carrier, respectively. The proband indicated by an arrow was used for CGH with the X-tiling array. Asterisks indicate persons having identical pCNVs among each family. A slash indicates that the person has died. NA, not available.

follows: arr Xp22.2 (11 680 788–12 313 191)×2 mat. FISH analysis revealed that the patient's mother (I-2) is a carrier but his unaffected sister (II-1) does not have the duplication (Supplementary Figure S1f). The carrier mother (I-2) showed a random X-inactivation pattern (Table 1).

MR494

The male proband (II-4) and his sister (II-2) were affected by moderate MR, and his brother (II-1) and another sister (II-3) had borderline MR (Figure 3). All his siblings had localization-related epilepsy in childhood. In the proband, an ~0.33-Mb duplication including *HDX* was detected at Xq21.1 (Supplementary Figure S4f). The aberration is as follows: arr Xq21.1 (83 463 344–84 006 214)×2 mat. FISH revealed that the unaffected mother (I-2), affected sister (II-2) and sister (II-3) with borderline MR had the same duplication, whereas the brother with borderline MR did not (Supplementary Figure S1g). The X-chromosome inactivation of the mother (I-2) had a random pattern and affected sister (II-2) and another sister (II-3) with borderline MR had a skewed pattern (Table 1).

MR86B

All three patients in the MR86B family had moderate MR. In the male proband (III-1), an ~0.18-Mb deletion was detected at Xq24 by aCGH (Figure 2). The aberration is as follows: arr Xq24 (120 358 756–120 574 498)×0 mat. This deletion contains no protein-coding genes but eight human expression sequence tags: DA381697, CB043836. CB043837, AW193789, AW894827, BF374258, AA191179 and AA789076 (Supplementary Figure S4g). The deletion was inherited from his affected grandmother and his affected mother (Supplementary Figure S1h). The X-chromosome inactivation showed a skewed pattern in the affected mother (II-2) and grandmother (I-2) (Table 1).

Detection of nine benign CNVs

We detected possible benign CNVs, which may not be associated with the MR phenotype, in nine regions based on our flowchart (Supplementary Table S1). Among them, one region containing several genes at Xp22.2 had not been registered in the DGV, and another region at Xq22.1 contains *protocadherin 19* (*PCDH19*, (OMIM 300460)), although its mutations have been reported to be related to female patients with MR (EFMR (OMIM 300088)).[22]

DISCUSSION

A duplication at Xq28 containing *MECP2* is one of the most common genomic rearrangements in neurodevelopmentally delayed male.[15] In this study, the duplication at Xq28 involving *MECP2* was detected in Japanese patients at high frequency (3/144=2.1%) compared with reported cases in Western countries (1/108=0.9%[13] or 1/54=1.9%[14]). The patients manifested several common phenotypes such as severe MR, muscular hypotonia, absence of speech and recurrent respiratory infections as reported.[15–19] Mapping at dup(X)(q28) of our three families indicated that the smallest region of overlap contained thirteen genes including *L1CAM* and *MECP2* (Supplementary Figure S4a), suggesting that these genes contribute to their

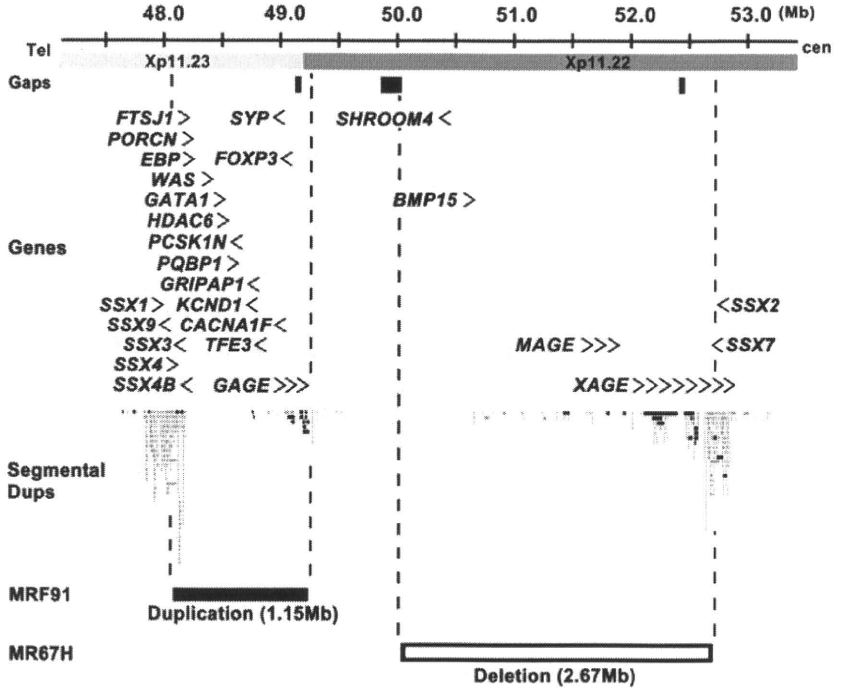

Figure 4 Mapping of aberrations at Xp11.23-p11.22 detected in families MRF91 and MR67H. Disease-associated and copy-number-sensitive genes (not drawn to scale) are described by chevrons. Gaps in the genome assembly, segmental duplications (Dups) are shown. Filled bars and gray bars indicate >99% similarity and 90–99% similarity, respectively, in segmental duplications. High-density oligonucleotide array (Agilent 244K) revealed an ~1.15-Mb duplication at Xp11.23 in MRF91 (filled bar) and an ~2.67-Mb deletion at Xp11.23-p11.22 in MR67H (open bar).

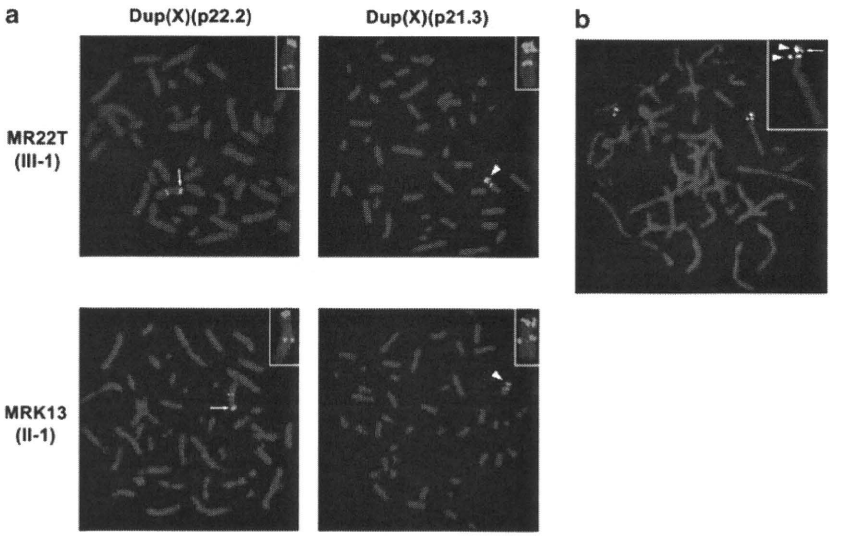

Figure 5 Duplicon at Xp21.3 were observed at Xp22.2 by FISH. (**a**) Representative results of FISH in probands of MR22T (upper) and MRK13 (lower). FISH using the clone RP11-2K15 at Xp22.2 (left column) and the clone RP11-438J7 at Xp21.3 (right column) showed strong green signals (arrows) and separate green signals (arrowheads), respectively, and the clone RP11-13M9 at Xq13.2 shows red signals as a reference in both experiments. An enlarged image of chromosome X is shown in the upper right insets in each panel. (**b**) Representative results of FISH in the patient's mother (I-2) in MRK13 with elongated metaphase chromosomes prepared as described elsewhere.[44] The clone RP11-2K15 at Xp22.2 and the clone RP11-438J7 at Xp21.3 demonstrated strong signals (red) and separate signals (green), respectively, in one allele. An enlarged image of the duplicated allele is shown in the upper right inset, indicating that the duplicated sequence at Xp22.2 was inserted in close proximity (arrow), whereas the duplicated sequence at Xp21.3 inserted into the duplication at Xp22.2 together with the original Xp21.3 (arrowheads). A full color version of this figure is available at *The Journal of Human Genetics* journal online.

phenotypes. Carvalho *et al.*[23] proposed the presence of low-copy repeats in the vicinity of the *MECP2* gene to be involved in the rearrangement including *MECP2*. In our cases, the distal breakpoints of all duplications were located on segmental duplications (Supplementary Figure S4a). In family MR347, interestingly, an ~182-kb deletion at Xp22.31 together with dup(X)(q28) were also detected in

two patients (III-1, III-2) showing strong autistic features and their carrier mother (II-2) (Supplementary Figure S4b). Although no protein-coding genes are located within the del(X)(p22.31), *NLGN4X* (OMIM 300427), which is known to be associated with autism,[24] is located near this region (~55 kb from the distal breakpoint), suggesting that this deletion may work as modifier for their phenotypes. In all mothers of the three families, the duplicated allele showed a late replication pattern dominantly (data not shown), indicating that they are not phenotypes due to the X-inactivation pattern. On the other hand, CNVs at autosomal region not registered in the DGV were detected in each of probands in three families (Supplementary Table S2). These CNVs contain protein-coding genes (*LPHN3*, *KIAA1370*, *MAP2K5* (OMIM 602520), *RSPO4* (OMIM 610573)). Although *RSPO4* are related to anonychia (OMIM 206800),[25,26] the proband of MR1P3 family having the deletion at this region has not shown anonychia and phenotypes have shown no difference among these three probands, suggesting that these CNVs were benign CNVs that have not been associated with the disease.

In the MRF91 family, an ~1.16-Mb duplication at Xp11.23 including *FTSJ1*, *PQBP1* and *SYP* was detected in the male proband (III-1), his affected younger sister (III-2) and their unaffected mother (II-2) (Figure 2; Supplementary Figure S1d). Duplications in the same region were reported in two males and six females of 2400 subjects (0.33%) with MR, speech delay and electroencephalographic anomalies.[27] Although electroencephalographic recordings have not been examined in the patients of family MRF91, phenotypic similarity, such as moderate MR and speech delay, among reported cases and our cases suggests genes located within this duplicated region to be associated with those phenotypes. This hypothesis is supported by higher expression of *FTSJ1* and *PQBP1* mRNAs in the male proband (III-1) compared with the carrier mother (II-2) and the affected sister (III-2) and in MRF91 family members having dup(X)(p11.23) compared with normal controls (Supplementary Figure S2). As dup(X)(p11.23) in both the sister (III-2) and mother (II-2) showed a late replicating pattern (Supplementary Figure S3), expression of *FTSJ1* and *PQBP1* with the duplication seems to be predominantly repressed by X-inactivation. However, *FTSJ1* expression in the affected sister (III-2) was lower than that in the carrier mother (II-2) but *PQBP1* expression showed the reverse (Supplementary Figure S2), suggesting that expression levels might not be perfectly reflected by X-inactivation status. *PQBP1* levels of proband (III-1), sister (III-2) and mother (II-2) with dup(X)(p11.23) were higher than the average +3 s.d. of 10 healthy controls, suggesting that *PQBP1* expression may be influenced by the duplication more strongly at least in LCLs. Nonsense mutations in *PQBP1* were detected in patients with MR and microcephaly.[28] It is noteworthy that our cases showed macrocephaly, suggesting that this phenotype results from increased *PQBP1* expression. In addition, excessive action of *PQBP1* has been shown to cause neuronal dysfunction,[29–33] indicating increased expression of *PQBP1* through duplication to be involved in MR with macrocephaly.

In the proband (III-1) of family MR67H, a novel ~2.67-Mb deletion at Xp11.23-p11.22 harboring *SHROOM4* (Figure 2). A missense exchange of *SHROOM4* was reported to segregate with Stocco dos Santos XLMR syndrome (OMIM 300434) in a large four-generation pedigree.[21] The affected males in the reported family presented with severe MR, delayed or no speech, seizures and hyperactivity. Our patient with null *SHROOM4* showed only moderate MR, suggesting that the missense exchange detected in Stocco dos Santos XLMR syndrome contributes to the pathogenesis of MR together with other phenotypes in a gain-of-function manner. Although genetic status in other members of the family was not investigated because of a lack of available materials, two of the proband's maternal uncles (II-2, II-3) had MR (Figure 3), suggesting that this deletion was inherited from the proband's mother (II-4) and probably contributes to MR. An oligonucleotide-array analysis revealed that breakpoints of dup(X)(p11.23) and del(X)(p11.22) were mapped within segmental duplications containing *SSX* genes, *GAGE* genes and *XAGE* genes and sequence gap, respectively (Figure 4). Previous reports[13,27] suggested that CNVs at Xp11.22-p11.23 were associated with flanking segmental duplications. In addition, broken forks are the precursor lesions directly processed into segmental duplications in yeast[34] and Fork Stalling and Template Switching (FoSTeS) has been proposed as a replication-based mechanism that produces nonrecurrent rearrangements potentially facilitated by the presence of segmental duplications.[35] Thus, the del(X)(p11.22) containing *SHROOM4* might occur through a segmental duplication-dependent manner.

We detected five novel candidate pCNVs, which have not been identified by similar screenings,[13,14] on the X chromosome in probands of five families, and each of their mothers had aberrations concordant with that detected in the proband. In MR22T and MRK13 families, we detected two identical duplications at Xp22.2 and Xp21.3 (Figure 2). FISH revealed that the duplicated sequence at Xp21.3 exists near the duplicated sequence at Xp22.2 (Figure 5), suggesting that these duplications were related to each other and occurred simultaneously. Thus, although large CNVs at Xp21.3 are registered in DGV (Supplementary Figure S4d), the duplication detected in this study is different from CNVs. The duplications showed complicated genomic rearrangements and the involvement of parts of genes (*REPS2*, *NHS* and *IL1RAPL1*). *IL1RAPL1* was identified as an XLMR gene. *REPS2* is associated with a small G protein and shows strong expression in brain tissue (LSBM, http://www.lsbm.org/index.html). As alterations in signaling pathways involving the Rho family of small GTPases contribute to both syndromic and nonsyndromic MR disorders[36] and mutation in the small GTPase gene *RAB39B* (OMIM300774) were identified in two MR patients,[37] it is possible that deregulated expression of *REPS2* contributes to MR. Protein-truncation mutations in *NHS* have been identified in patients with Nance-Horan syndrome (OMIM 302350), an X-linked developmental disorder characterized by congenital cataracts, dental anomalies, facial dysmorphism and MR in some cases. As our patients in both families did not have cataracts or dental anomalies, the genomic rearrangement involved in *NHS* may not affect the function of this gene. Although the characteristic CNVs observed in two patients of two unrelated families were identical, the severity of MR was different between patients: one patient had severe MR but the other had moderate MR, suggesting this complicated genomic rearrangement to vary in penetrance among individuals. It has not yet been clarified whether the complex CNV was transmitted from a single founder or occurred independently. Further analysis such as genomic DNA sequencing and/or screening among different ethnic groups will be needed to disclose the full details of it.

In family MR1WK, an ~632-kb duplication at Xp22.2 was detected in the affected son (II-2) and unaffected mother (I-2), indicating that it was segregated with the disorder (Figure 2; Supplementary Figure S1f). The duplicated region includes *MSL3* and a part of *FRMPD4* (Supplementary Figure S4e). *MSL3* was identified as a human homolog of *Drosophila* male-specific lethal 3 (msl3) and expressed ubiquitously in adult tissues.[38] The expression level of *MSL3* was not increased in the proband with the duplication (data not shown). *FRMPD4* showed a high expression level specifically in human brain tissue (LSBM), and contains one PDZ domain, a protein-interaction domain frequently found in multidomain scaffolding proteins,